JPE 3-1-5

Self-Commissioning for Surface-Mounted Permanent Magnet Synchronous Motors

Naomitsu Urasaki*, Tomonobu Senjyu, and Katsumi Uezato

Dept. of Electrical and Electronics Eng., The University of the Ryukyus, Okinawa, Japan

ABSTRACT

This paper presents the self-commissioning for surface-mounted permanent magnet synchronous motor. The proposed strategy executes three tests with a vector controlled inverter drive system. To do this, synchronous *d-q* axes currents are appropriately controlled for each test. From the three tests, armature resistance, armature inductance, equivalent iron loss resistance, and emf coefficient are identified automatically. The validity of the proposed strategy is confirmed by experimental results.

Keywords: self-commissioning, parameter identification, surface-mounted permanent magnet synchronous motor

1. Introduction

Recently, sensorless control, high efficiency control, flux weakening control, and iron loss compensation control for inverter fed vector controlled surface-permanent magnet synchronous motor (SPMSM) drive have widely been developed. These control methods strongly depend on the electrical parameters. Then, these parameters should be identified in advance. However, it spends much time and energy trying to identify parameters by manual operations. In addition, it may be a difficult task to measure parameters due to constrains for installation location and/or utilization of measuring instrument. An inverter with self-commissioning solves the problems, i.e. the parameters are automatically identified at start-up stage.

Manuscript received April 1, 2002; revised Nov. 30, 2002.

Corresponding Author: urasaki@tec.u-ryukyu.ac.jp Tel: +81-98-895-8710, Fax: +81-98-895-8708

For this reason, self- commissioning strategies have been attracted attention[1][2]. Another solution for this problem is to identify parameters on-line[3]. On-line parameter identification method has the advantage that the parameters are identified adaptively corresponding to operating points. However, it may be difficult to identify a number of parameters.

This paper proposes a self-commissioning for SPMSM. The proposed self-commissioning consists of three tests, i.e., dc test, single-phase ac test, and synchronous drive test. To automatically realize these tests with using a vector controlled inverter drive system, synchronous *d-q* axes currents are appropriately controlled for each test. Since all the electrical parameters except for the emf constant are measured in standstill, the implementation of the proposed method is simple. Furthermore, the iron loss resistance can also be identified. Thus, the proposed method is suitable for the vector control strategies considering iron loss. The automatic identification results are experimentally compared with the measurement results by manual operations.

2. Formulation of SPMSM Taking Iron Loss Into Account

In the synchronous reference frame (d-q axes), the voltage equation for SPMSM is expressed as,

$$\left.\begin{aligned} v_d &= Ri_d + p\psi_d - \omega_r\psi_q \\ v_q &= Ri_q + p\psi_q - \omega_r\psi_d \end{aligned}\right\} \quad (1)$$

where, v_{dq}, i_{dq}, and ψ_{dq} are the d-q axes stator voltages, currents, and stator flux linkages, respectively, R, ω_r, and p are the armature resistance, rotor electrical angular velocity, and differential operator ($=d/dt$), respectively. The stator flux linkages are expressed as,

$$\left.R_m = \frac{\omega_r^2 M_{13}^2}{R_3^2 + \omega_r^2 L_3^2} R_3\right\} \quad (2)$$

where, L and K_e are the armature inductance and emf coefficient, respectively. The d-q axes equivalent circuit for SPMSM is shown in Fig. 1.

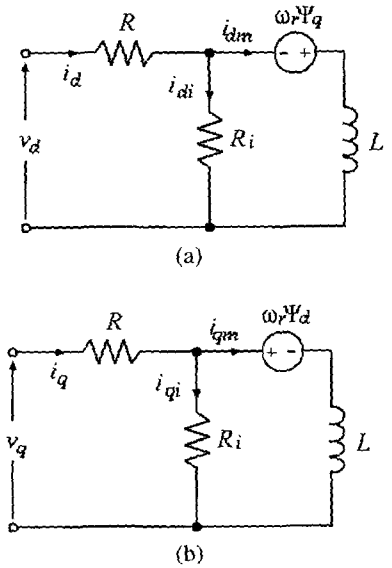

Fig. 1. d-q axes equivalent circuit for SPMSM: (a) d-axis, (b) q-axis.

3. Self-Commissioning Strategy

The automatic identifications of electrical parameters of SPMSM are implemented from a series of an individual test.

The series contain the dc test, single-phase ac test, and synchronous drive test.

3.1 DC Test

When a dc voltage is applied to the SPMSM as shown in Fig. 2, the SPMSM stops at the rotor position $\theta_r = 0$ ($\omega_r = 0$). In this case, the relationships between the applied dc current/voltage and the phase current/voltage become as follows:

$$\left.\begin{aligned} i_a &= I_{DC}, & i_b &= i_c = -\tfrac{1}{2} I_{DC} \\ v_a &= \tfrac{2}{3} V_{DC} & v_b &= v_c = -\tfrac{1}{3} V_{DC} \end{aligned}\right\} \quad (3)$$

Transforming the three-phase quantities into the synchronous d-q quantities with using the transformation matrix:

$$[C] = \sqrt{\frac{2}{3}} \begin{bmatrix} \cos\theta_r & \cos(\theta_r - \frac{2}{3}\pi) & \cos(\theta_r + \frac{2}{3}\pi) \\ -\sin\theta_r & -\sin(\theta_r - \frac{2}{3}\pi) & -\sin(\theta_r + \frac{2}{3}\pi) \end{bmatrix} \quad (4)$$

We obtain the d-q axes current and voltage as,

$$\left.\begin{aligned} i_d &= \sqrt{\tfrac{3}{2}} I_{DC}, & i_q &= 0 \\ v_d &= \sqrt{\tfrac{2}{3}} V_{DC} & v_q &= 0 \end{aligned}\right\} \quad (5)$$

Accordingly, the d-q axes equivalent circuit is expressed as shown in Fig. 3. It follows from Fig. 3(a) that the d-axis impedance $\dot{Z}_d^{DC}$ is equal to the armature resistance R. Since $\dot{Z}_d^{DC} = \dot{V}_d / \dot{I}_d$, the armature resistance is calculated as,

$$R = \frac{2}{3}\frac{V_{DC}}{I_{DC}} \quad (6)$$

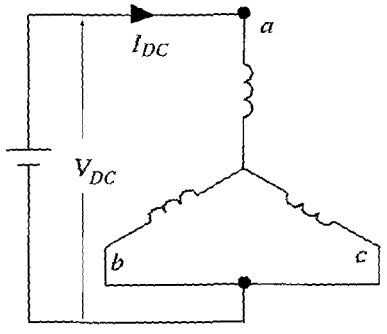

Fig. 2. DC test topology.

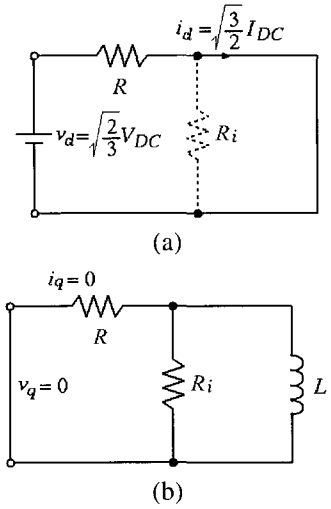

Fig. 3. d-q axes equivalent circuit under dc test: (a) d-axis, (b) q-axis.

3.2 Single-Phase AC Test

When a single-phase ac voltage is applied to the SPMSM as shown in Fig. 4, the SPMSM stops at $\theta_r = 0$ ($\omega_r = 0$). In this case, the relationships between the applied ac current/voltage and phase current/voltage becomes as follows:

$$\left.\begin{aligned} i_a &= i_{AC}, & i_b &= i_c = -\tfrac{1}{2} i_{AC} \\ v_a &= \tfrac{2}{3} v_{AC} & v_b &= v_c = -\tfrac{1}{3} v_{AC} \end{aligned}\right\} \tag{7}$$

Transforming the three-phase quantities into the synchronous d-q quantities with using (4), we obtain the d-q axes currents and voltages as,

$$\left.\begin{aligned} i_d &= \sqrt{\tfrac{3}{2}} i_{AC}, & i_q &= 0 \\ v_d &= \sqrt{\tfrac{2}{3}} v_{AC} & v_q &= 0 \end{aligned}\right\} \tag{8}$$

Accordingly, the d-q axes equivalent circuit is expressed as shown in Fig. 5. Then, the d-axis impedance is derived as,

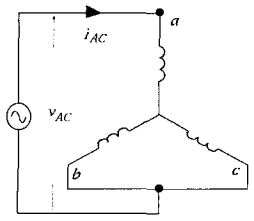

Fig. 4. Single-phase ac test topology.

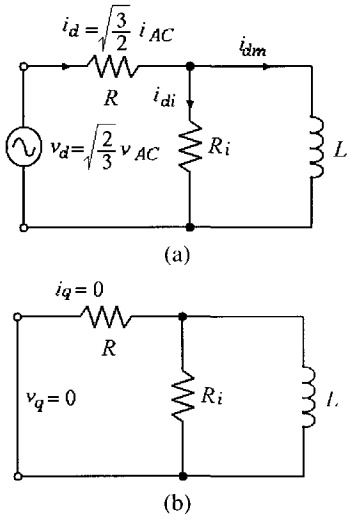

Fig. 5. d-q axes equivalent circuit under single-phase ac test: (a) d-axis, (b) q-axis.

$$\dot{Z}_d^{AC} = R + \frac{R_i(\omega_e L)^2}{R_i^2 + (\omega_e L)^2} + j\frac{R_i^2 \omega_e L}{R_i^2 + (\omega_e L)^2} \tag{9}$$

where, ω_e is the angular frequency of the applied voltage. The following relation: [4]

$$\left(\frac{\omega_e L}{R_i}\right)^2 << 1 \tag{10}$$

simplifies the impedance as,

$$\dot{Z}_d^{AC} = R + \frac{(\omega_e L)^2}{R_i} + j\omega_e L \tag{11}$$

Since $\dot{Z}_d^{AC} = \dot{V}_d / \dot{I}_d$, the relationship between the applied voltage and line current is derived as,

$$\dot{V}_{AC} = \frac{3}{2} \dot{Z}_d^{AC} \dot{I}_{AC} \tag{12}$$

Then, the apparent power is expressed as,

$$\dot{S}_{AC} = \frac{3}{2}\left(R + \frac{\omega_e^2 L^2}{R_i}\right) I_{AC}^2 + j\frac{3}{2}\omega_e L I_{AC}^2 \tag{13}$$

where, the first and second terms in the right-hand side correspond to the active power P_{AC} and reactive power Q_{AC}, respectively. From the second term in (13), the armature inductance is identified as.

$$L = \frac{2}{3}\frac{Q_{AC}}{\omega_e I_{AC}^2} \tag{14}$$

Similarly, the iron loss resistance is calculated from the first term in (13) as,

$$R_i = \frac{(\omega_e L)^2}{\frac{2}{3}\frac{P_{AC}}{I_{AC}^2} - R} \tag{15}$$

3.3 Synchronous Drive Test

The synchronous drive test topology is shown in Fig. 6. The geometry is normal for the three phase ac machines. When a three-phase voltage is applied to the SPMSM, the SPMSM synchronously rotates with applied angular frequency ($\omega_r = \omega_e$). In steady state condition (p=0), the d-q axes equivalent circuit is expressed as shown in Fig. 7. Then, (2) is rearranged as,

$$\left.\begin{aligned} \psi_d &= Li_d + K_e + \frac{\omega_e L}{R_i} Li_q \\ \psi_q &= Li_q - \frac{\omega_e L}{R_i}(Li_q + K_e) \end{aligned}\right\} \tag{16}$$

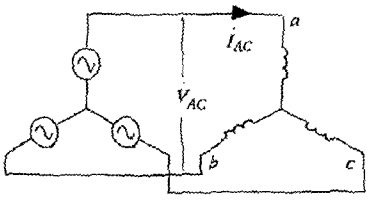

Fig. 6. Synchronous drive topology.

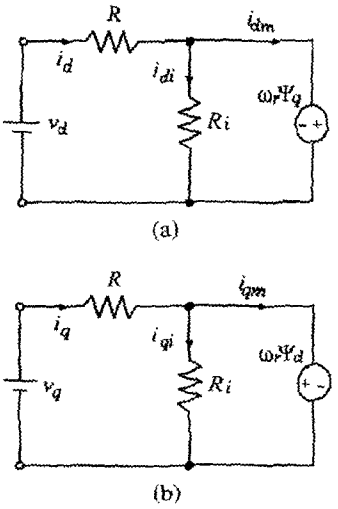

Fig. 7. d-q axes equivalent circuit under synchronous drive test: (a) d-axis, (b) q-axis.

In steady state condition (p=0), substituting (16) into (1) gives the voltage equation expressed in the form:

$$\begin{bmatrix} v_d \\ v_q \end{bmatrix} = \begin{bmatrix} R + \frac{(\omega_e L)^2}{R_i} & -\omega_e L \\ \omega_e L & R + \frac{(\omega_e L)^2}{R_i} \end{bmatrix} \begin{bmatrix} i_d \\ i_q \end{bmatrix} + \omega_e K_e \begin{bmatrix} \frac{\omega_e L}{R_i} \\ 1 \end{bmatrix} \tag{17}$$

Since the impedance matrix in the first term is constant as long as the applied angular frequency is constant, the terminal voltage is proportion to the line current. Especially, when the line current is zero (i_d=i_q=0), the terminal voltage is equal to the electromotive force, i.e.,

$$\begin{bmatrix} v_d \\ v_q \end{bmatrix} = \omega_e K_e \begin{bmatrix} \frac{\omega_e L}{R_i} \\ 1 \end{bmatrix} \tag{18}$$

Accordingly, the emf constant K_e is calculated as,

$$K_e = \frac{V_{AC}}{\omega_e} \tag{19}$$

where $V_{AC}(=\sqrt{v_d^2 + v_q^2})$ is the rms of the terminal voltage. It is noted that (10) is applied to the derivation of (19).

3.4 Current Control

In order to implement the self-commissioning strategy with vector controlled inverter drive system, the phase current should be appropriately commutated according to each test. To do this, the synchronous d-q axes current controller shown in Fig. 8 is constructed in this paper. For instance, when the d-q axes current commands (i_d^*, i_q^*) are set to (5), the dc test is realized.

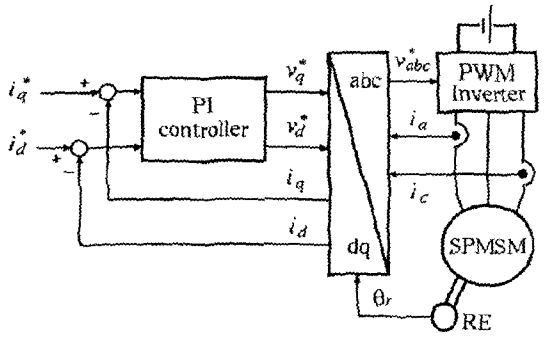

Fig. 8. Current control system.

3.5 Computation of Current, Voltage, and Power

In general, current sensors are installed in the vector-controlled inverter. Then, the instantaneous current information is easily available from the current sensor. However, the acquirement of the instantaneous voltage information is difficult because the inverter output voltage is pulse waveform. For this reason, the voltage command of the inverter is substituted for the instantaneous voltage information. The dc current I_{DC}, dc voltage V_{DC}, rms of ac current I_{AC}, rms of ac voltage V_{AC}, active power P_{AC}, and reactive power Q_{AC} are computed with using the instantaneous current and voltage command information as follows:

$$I_{DC} = \frac{1}{N}\sum_{k=1}^{N} i_{DC}(k) \tag{20}$$

$$V_{DC} = \frac{1}{N}\sum_{k=1}^{N} v_{DC}^{*}(k) \tag{21}$$

$$I_{AC} = \sqrt{\frac{1}{N}\sum_{k=1}^{N} i_{AC}^{2}(k)} \tag{22}$$

$$V_{AC} = \sqrt{\frac{1}{N}\sum_{k=1}^{N} v_{AC}^{*2}(k)} \tag{23}$$

$$P_{AC} = \frac{1}{N}\sum_{k=1}^{N} i_{AC}(k)v_{AC}^{*}(k) \tag{24}$$

$$Q_{AC} = \sqrt{(V_{AC}I_{AC})^2 - P_{AC}^2} \tag{25}$$

where, $i_{DC}(k)$, $i_{AC}(k)$ are the detected currents at instant k, $v_{DC}^{*}(k)$, $v_{AC}^{*}(k)$ are the voltage commands at instant k, and N is the number of data during a period.

3.6 Influence of Switching Device Nonlinearity

The difference between the voltage command and actual voltage is essentially inevitable because the switching device of inverter has nonlinear characteristics due to the dead time and voltage drop. To compensate the influence of the voltage error on the computation of (21), (23), and (24), the voltage errors have been measured in advance. Figs. 9 to 12 show the differences between the voltage command and actual voltage detected with the digital power meter (DPM) for each test and the difference between the calculated active power and the actual one with DPM. These characteristics are utilized in the correction of the voltage command.

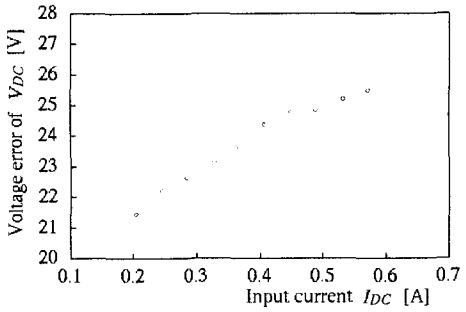

Fig. 9. Voltage error for dc test.

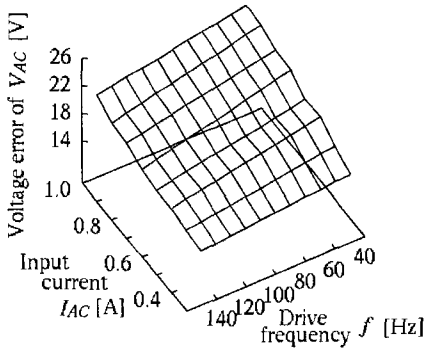

Fig. 10. Voltage error for single-phase ac test.

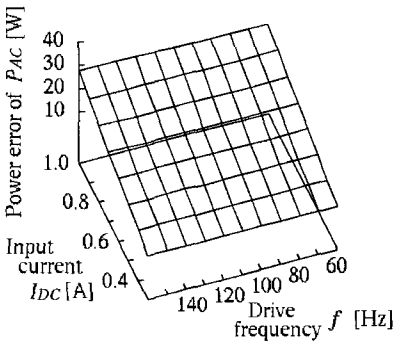

Fig. 11. Power error for single-phase ac test.

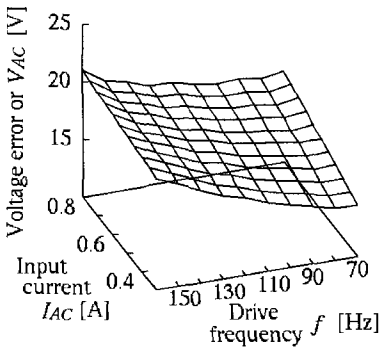

Fig. 12. Voltage error for synchronous test.

4. Identification Results

To realize the dc test, single-phase ac test, and synchronous drive test, the current control system in Fig. 8 is incorporated into the vector controlled inverter drive system. Table 1 shows the specification of the tested SPMSM.

Table 1. Specifications of tested SPMSM.

Rated power	30 W
Rated current	3.0A
Rated torque	0.19N•m
Rated speed	1500 rpm
Number of pole-pairs	8

4.1 DC Test

Fig. 13 shows the current control result for dc test. It can be confirmed from this figure that the line current is dc quantity. The identification result of the armature resistance R with using (6) is shown in Table 2. It almost agrees with the measured one with DPM.

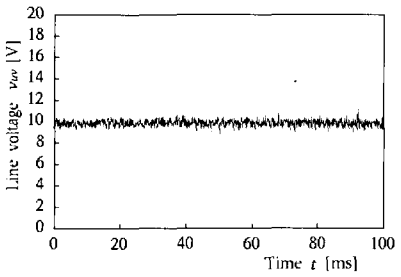

Fig. 13. Control result of dc current.

Table 2. Self-commissioning results.

Parameter	SC	DPM	Error
R [Ω]	7.86	7.66	2.6%
L [H]	0.024	0.022	9.1%
R_i [Ω]	180	172	4.6%
K_e [V•s/rad]	0.049	0.047	4.3%

4.2 Single-Phase AC Test

Fig. 14 shows the current control result for the single-phase ac test. It can be confirmed that the line current waveform is sinusoidal. The identification results of the armature inductance L with using (14) and the iron loss resistance R_i with using (15) for various applied frequency are shown in Figs. 15 and 16, respectively.

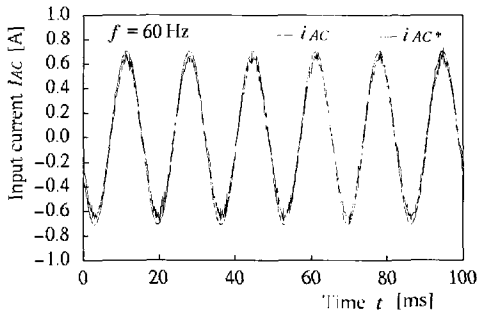

Fig. 14. Control result of single-phase ac current.

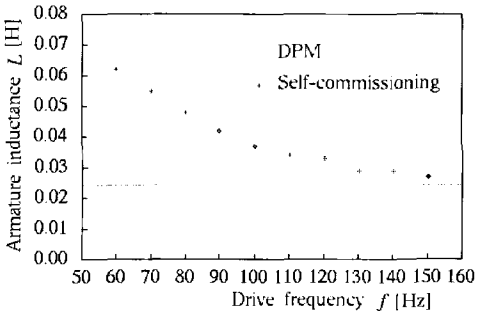

Fig. 15. Armature inductance.

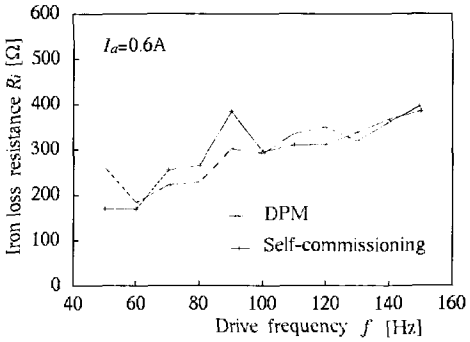

Fig. 16. Iron loss resistance.

It follows from Fig. 15 that the armature inductance identified by the proposed self-commissioning strategy agrees well with the measured one with DPM. The obtained armature inductance increases with decreasing driving frequency because the ratio of the harmonic RMS increases in low frequency. The numerical results at 150Hz are listed in Table 2. It follows from Fig. 16 that the iron loss resistance identified by the proposed strategy almost agrees with the measure one with DPM. However, the tested SPMSM is a small machine, that is, the iron loss is comparatively small. Then, either the identified and measured iron loss resistances are scattering. The numerical results at 60Hz are listed in Table 2.

4.3 Synchronous drive test

Fig. 17 shows the terminal voltage versus line current for the synchronous drive test at ω_r = 300π rad/s (f=150Hz). Since the characteristic is linear, the terminal voltage when the line current is zero, i.e., electromotive force is easily estimated. The identification result of the emf constant K_e with using (19) is listed in Table 2. The identified emf constant agrees well with the measured one by the no-load generating test.

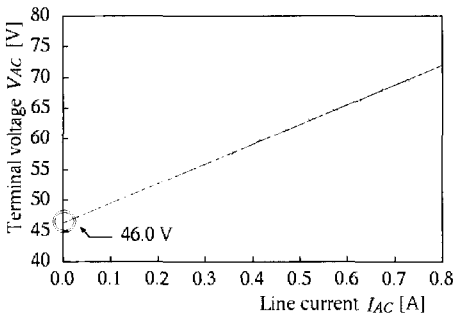

Fig. 17. Terminal voltage vs. line current under constant speed.

5. Conclusions

This paper proposes the self-commissioning for SPMSM. The dc test, single-phase ac test, and synchronous drive test are executed based on the synchronous d-q axis current controller incorporated in the vector controlled inverter drive system. The automatic identification parameters almost agree with the measurement one by the manual operations. The identification errors are with in 10%. In order to improve the precision of identification, a dead-time effect of inverter should be compensated strictly.

References

[1] Y.N. Lin and C.L. Chen, "Automatic IM parameter measurement under sensorless field-oriented control", IEEE Trans. Ind. Electron., Vol. 46, No. 1, pp. 111~118, Feb. 1999.

[2] Y.S. Lai, J.C. Lin, and J.J. Wang, "Direct torque control induction motor drives with self-commissioning based on Taguchi methodology", IEEE Trans. Power Electron., Vol. 15, No. 6, pp. 1065~1071, Nov. 2000.

[3] S. Bolognani, M. Zigliotto, and K. Unterkofler, "On-line parameter commissioning in sensorless PMSM drives", in Proc. ISIE '97, pp. 480~484, 1997.

[4] N. Urasaki, T. Senjyu, and K. Uezato, "An accurate modeling for permanent magnet synchronous motor drives", in Proc. APEC 2000, pp. 387~392, New Orleans, 2000.

Naomitsu Urasaki was born in Okinawa Prefecture, Japan in 1973. He received the B.S. and M.S. degrees in electrical engineering from University of the Ryukyus, Japan, in 1996 and 1998, respectively. Since 1998, he has been with Department of Electrical and Electronics Engineering, Faculty of Engineering, University of the Ryukyus, where he is currently a Research Associate. His research interests are in the areas of modeling and control of ac motors. Mr. Urasaki is a Member of the Institute of Electrical Engineers of Japan.

Tomonobu Senjyu was born in Saga Prefecture, Japan, in 1963. He received the B.S. and M.S. degrees in electrical engineering from the University of the Ryukyus, Okinawa, Japan, in 1986 and 1988, respectively, and the Ph.D. degree in electrical engineering from Nagoya University, Nagoya, Japan, in 1944. Since 1988, he has been with the Department of Electrical and Electronics Engineering, Faculty of Engineering, University of the Ryukyus, where he is currently a professor. His research interests are in the areas of stability of ac machines, advanced control of electrical machines, and power electronics. Prof. Senjyu is a member of the Institute of Electrical Engineers of Japan.

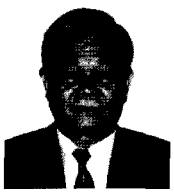

Katsumi Uezato was born in Okinawa Prefecture, Japan, in 1940. He received the B.S. degrees in electrical engineering from the University of the Ryukyus, Okinawa, Japan, in 1963, the M.S. degree in electrical engineering from Kagoshima University, Kagoshima, Japan, in 1983. Since 1972, he has been with the Department of Electrical and Electronics Engineering, Faculty of Engineering, University of the Ryukyus, where he is currently a Professor. He is engaged in research on stability and control of synchronous machines. Prof. Uezato is a member of the Institute of Electrical Engineers of Japan.